Proceedings World Geothermal Congress 2020+1
Reykjavik, Iceland, April - October 2021

Performance of Ground Source Heat Pumps in Densely Populated Areas

Fascì M.L[1], Lazzarotto A. [1], Coronado M., Claesson J. [1]

[1]KTH Royal Institute of Technology - Department of Energy Technology, Brinellvägen 68 (Stockholm)

mlfasci@kth.se

Keywords: Ground source heat pumps, neighbouring boreholes, thermal influence, heat pump performance

ABSTRACT

Ground source heat pumps (GSHPs) connected to vertical borehole heat exchangers (BHEs) are a popular technology to provide heat and/or refrigeration in residential and commercial buildings. When such systems only extract/reject heat from/to the ground, the temperature in the ground surrounding the BHEs decreases/increases until it reaches a steady state. How fast the steady state temperature is reached and how different it is from the undisturbed temperature depends on many factors; one factor is the presence of neighbouring GSHPs. As the number of neighbouring systems increases, the steady state condition is reached more slowly and the magnitude of the temperature change in the ground increases. If designed without taking into account the presence of neighbouring installations, the actual temperature change in the ground surrounding the BHE(s) of a GSHP might be significantly higher than the forecasted temperature change in the ground; meaning that the actual performance of the heat pump (HP) would be lower than the expected performance. In this article, we show a methodology to evaluate the performance of a GSHP in a densely populated area and subsequently use it to evaluate how the performance of GSHPs are affected by the presence of neighbouring installations in a densely populated area used as a case study.

1. INTRODUCTION

Ground source heat pumps (GSHPs) are one of the most efficient ways to provide space heating/cooling and domestic hot water. A GSHP mainly consists of a ground heat exchanger and a heat pump (HP) unit. The ground heat exchanger extracts/ rejects heat from/to the underground; it usually consists of one or several vertical boreholes fitted with closed-loop u-tubes in which a heat carrier fluid is circulated. After circulating in the borehole heat exchanger(s) (BHEs), the heat carrier fluid is used as a heat source/sink in the evaporator/condenser of the heat pump, which, at the expense of electrical power, lifts/lowers the temperature of the heat to the desired temperature for the distribution system.

GSHPs began to spread during the oil crisis of the ’70s due to their cost-effectiveness compared to boilers (most used solution at that time) and have kept increasing in number during the last five decades (Sanner, 2016). In Sweden, for example, around 1 out of 5 single family houses uses a GSHP for space heating and domestic hot water (Gehlin and Andersson, 2016).

As the number of GSHP installations in an area increases, the underground temperature in that area might change significantly due to their operation. In fact, when a BHE extracts/rejects heat from/to the underground, the temperature of the ground immediately surrounding the BHE decreases/increases. If a GSHP operates mostly in heating/cooling mode, i.e., the thermal load on the underground is unbalanced, the temperature further away from the BHE will also change. Moreover, as the number of installations increases the heat extracted/rejected increases as well, and so the underground temperature change.

The underground temperature is an extremely important factor for the performance of a GSHP. In fact, as the the underground temperature decreases/increases, the coefficient of performance (COP) decreases depending if the GSHP operates in heating/cooling mode. As a matter of fact, Staffell at al. (2012) analyzed several heat pump catalogues and found that the COP drops by between 0.6 and 1.0 for every 10 K increase in the temperature lift of a HP, giving 0.6–1.0 kW less heat output per kW of electrical input.

Consequently, a GSHP with unbalanced load has worse performance if surrounded by installations having similar operating conditions and therefore aggravating the temperature change in the underground.

In the last years, researchers have started studying the effects of a high density of GSHPs in a neighbourhood. Miglani et al. (2018) proposed a geographical information system (GIS) methodology to size and position the boreholes in an urban area where several buildings are equipped with GSHPs. Their methodology takes into account the thermal interference between neighbouring boreholes using the finite line source (FLS) model, and estimates the sustainable geothermal energy potential (GEP) in the area. They also estimated the effect of the interactions between neighbouring systems on the GEP of a neighbourhood in Zurich. Choi et al. (2018) coupled a dynamic building simulation to a numerical BHE model to simulate a scenario with high density of GSHPs in Tokyo. In their case study, the heat injection load of each borehole was twice as high as the heat extraction load. They found out that the temperature in the ground would rise of 7 K compared to the initial ground temperature after 10 years of operation, deteriorating the performance of the HP during the cooling periods. Witte (2018) proposed a method based on the Infinite line source (ILS) model to assess the interactions between neighbouring small GSHPs. He used the model to compute the temperature disturbances between neighbouring boreholes at several distances after given times and simplified the results in nomograms. Fascì and Lazzarotto (2019) proposed a model based on the stacked finite line source (SFLS) to estimate the thermal influence between neighbouring borehole heat exchangers in a densely populated area. Fascì et al. (2019) proposed a method based on the FLS to estimate the thermal influence between neighbouring borehole heat exchangers in a densely populated area and to evaluate different strategies to reduce it.

However, there seems to be missing a study dedicated to the evaluation of the performance of GSHPs in densely populated areas, to the best of our knowledge. Koohi-Fayegh and Rosen (2013) proposed an analytical model to evaluate the change of performance of a GSHP affected by the presence of neighbouring installations. Their model takes into account the heat transfer inside and outside

the borehole and evaluates the performance in terms of COP of Carnot. However, they applied the model to only two neighbouring borehole heat exchangers that operate with perfectly balanced load during the year.

In this paper, we describe a simple methodology to simulate a GSHP system. We apply this methodology to a specific case study where the GSHP is used only for heating and evaluate the difference between the performances of an isolated GSHP and the same GSHP in an area with high density of identical GSHPs. We demonstrate how the presence of neighbouring systems affects the temperature of the heat source and consequently the COP of the system, the heat delivered by the HP and the electricity consumption of the HP and the auxiliary system used as a backup. We also show the trend of the heat extraction from the BHE(s). The results are related to the case study considered, however the methodology used, that we implemented in the open source language Julia (Bezanson et al., 2017), can be easily implemented to find results related to different case studies.

2. METHODOLOGY

The aim of this paper is to show the difference between the performances of an isolated GSHP and the same GSHP in an area with high density of identical GSHPs. For this purpose, we created two different scenarios:

A. **Scenario A**: we considered only one GSHP installation. To evaluate the performance of the system, we modelled the HP itself, the load that the HP was required to satisfy (temperature and thermal power) with hourly resolution, and the temperature of the heat source of the heat pump, i.e., the secondary fluid temperature, directly related to the underground temperature.
B. **Scenario B:** we considered an indefinitely extended neighbourhood where all the houses and GSHP installations share the same characteristics. The same models as in Scenario A were used for the HP, the HP load and the secondary fluid temperature. However, a different model, taking into account also the influence of the neighbouring boreholes was used to evaluate the underground temperature.

2.1 Scenario A: isolated GSHP

2.1.1 Heat pump model

Concerning the heat pump model, the choice was between:

a) a black box model, based on interpolation and extrapolation of the performance map[1] given in the catalogue data;
b) a model based on the thermodynamic principles governing the heat pump.

We excluded the black box model because extrapolation of the heat pump performance out of the range given by the manufacturer leads to less accurate results (Jin and Spitler, 2002; Scarpa et al., 2012). Therefore, we chose a commercial HP and modelled each of the components considering the refrigerant cycle and the underlying thermodynamic principles. However, this required the knowledge of several parameters[2] not given by the manufacturer in the HP catalogue data. Therefore, we used the methodologies described by Jin and Spitler (2002) and Cimmino and Wetter (2017) to estimate such parameters from the data given by the manufacturer. This consisted in solving a multi-variable optimization problem. The catalogue data used as input and the parameters obtained through the optimization procedure are shown in the Appendix. The methodology described by Cimmino and Wetter (2017) was used to model the HP. More details about how we implemented the models to find the parameters and to evaluate the performance of the heat pump are described by Coronado (2019). The necessary inputs to run this HP model and obtain the heating capacity $\dot{Q}_{HP}$ and the compressor power $\dot{W}$ are the temperature of the water at the inlet of the condenser (see *2.1.2 Load model*) and the temperature of the secondary fluid at the inlet of the evaporator (see *2.1.3 Heat source model*). From the outputs of the HP model we calculated the coefficient of performance (COP) of the HP and the ratio $\frac{\dot{Q}_{load}}{\dot{Q}_{HP}}$, where $\dot{Q}_{load}$ is the heating load of the house. This ratio determines the fraction of the hour during which the HP is on. A ratio larger than 1 means that the HP is not able to satisfy the building load, and auxiliary heating is needed. $\dot{Q}_{load} - \dot{Q}_{HP}$ is the auxiliary heating needed. An additional output of the HP model is the heat exchanged at the evaporator, which is assumed to be equal to the heat extracted from the borehole. This is an input for the heat source model (see *2.1.3 Heat source model*).

2.1.2 Load model

Concerning the heat pump load, we assumed an annual load equal to the space heating load of an average Swedish single-family house (neglecting hot water production). A simple linear model was then used to evaluate the hourly load $\dot{Q}_{load}$. This was considered proportional to the difference between the ambient temperature and a base temperature set equal to 15.5 °C. Additional details concerning the evaluation of the house load are available in Fascì et al. (2018). The house load was the load imposed at the condenser of the heat pump and satisfied by the heat pump only, when possible, or by a combination of heat pump and auxiliary heating.

The temperature of the water at the inlet of the condenser, corresponding to the return temperature from the house, was calculated through the following procedure:

1. The heat delivered by the radiators to the house (equal to the heat load of the house) can be expressed as:

$$\dot{Q}_{load} = \mathrm{UA}_{rad} \cdot \left(\overline{T_{avg}} - T_{room}\right) = C\left(\overline{T_{avg}} - T_{room}\right)^{n+1} \quad (1)$$

$$\dot{Q}_{load} = \dot{m}_w \cdot c_{p,w} \cdot (T_s - T_r) \quad (2)$$

[1] Heating capacity and electric consumption as a function of the temperatures of the heat source and heat sink
[2] Nominal refrigerant volume flow rate, built in volume ratio between discharge and suction of the compressor, leakage coefficient of the compressor, degree of superheating, electromechanical efficiency of the compressor, constant part of the power losses, heat transfer coefficients UA_{eva} and UA_{cond} of evaporator and condenser.

Where UA_{rad} is the heat transfer coefficient of the radiators, $\overline{T_{avg}}$ is the mean temperature of the radiator wall plates, i.e., average between the supply temperature to the radiator T_s and return temperature from the radiators T_r, T_{room} is the temperature of the room, set equal to 20 °C, C is a constant to be evaluated, n is the coefficient for natural convection set equal to $\frac{1}{3}$, and $\dot{m}_w$ and $c_{p,w}$ are respectively the water flow rate in the radiators and its specific heat.

2. The constant C and the mass flow rate $\dot{m}_w$ were evaluated applying the design conditions of the distribution system respectively to equations 1 and 2. The design conditions correspond to: $\dot{Q}_{load}$ being the house load when the outdoor temperature is equal to -17 °C, T_s = 45 °C, T_r = 35 °C.
3. Knowing C and $\dot{m}_w$, T_r was calculated as function of the house heat load. The expression to calculate T_r was derived from equations 1 and 2. It is:

$$T_r = \left(\frac{\dot{Q}_{load}}{C}\right)^{\frac{1}{n+1}} - \frac{\dot{Q}_{load}}{2\,\dot{m}_w \cdot c_{p,w}} + T_{room} \qquad (3)$$

The house load and T_r are independent of the heat pump and heat source models.

2.1.3 Heat source model

The heat source for the evaporator of the heat pump is the secondary fluid circulating inside the borehole. The temperature of the secondary fluid at the exit of the BHE, i.e., entrance of the evaporator, is together with T_r an input for the HP model. It was calculated as described by Javed and Spitler (2016):

$$T_{sf}(t_n) = T_b(t_n) - \frac{q(t_n)}{R_b^*} + \frac{q(t_n)}{2\dot{m}_{sf}, c_{p,sf}} \qquad (4)$$

Where at time t_n, T_b is the underground temperature at the borehole wall, q is the linear heat extraction from the BHE, $\dot{m}_{sf}$, is the mass flow rate of the secondary fluid, $c_{p,sf}$ is the heat capacity of the secondary fluid, $R_b^*$is the effective borehole resistance. $R_b^* = 0.07\ m \cdot K/W$ was set as a constant value for the borehole resistance; this value falls within the typical range of borehole thermal resistances measured in Sweden (Javed and Spitler, 2016).

The temperature at the borehole wall was calculated using the finite line source (FLS) model (Spitler and Bernier, 2016), i.e., the average temperature drop at time *t*, over the wall of a BHE of radius *r*, long *H* and buried at a depth *D*, due to a constant linear heat extraction q from the BHE itself can be expressed as:

$$\overline{\Delta T}(t) = \frac{q}{2\pi k} \cdot \big(\theta(\alpha, r, t, H, 0) - \theta(\alpha, r, t, H, H + 2D)\big) = \frac{q}{2\pi k} \cdot fls(\alpha, r,\ t, H, D) \qquad (5)$$

With:

$$\theta(\alpha, r, t, H, \Delta z) = \frac{1}{2H}\int_{\frac{1}{\sqrt{4\alpha t}}}^{\infty} \frac{1}{s^2} exp(-r^2 s^2) \left[\begin{matrix} ierf\big((\Delta z + H)s\big) - ierf\big((\Delta z - H)s\big) + \\ -2ierf(s\Delta z) \end{matrix}\right] ds \qquad (6)$$

$$ierf(X) = Xerf(X) - \frac{1}{\sqrt{\pi}}(1 - e^{-x^2}) \qquad (7)$$

where *k* is the ground conductivity, α the ground diffusivity and *erf* the error function.

Equation 5 is valid in case of constant heat extraction. Since the heat extraction from the borehole varies with time, superposition in time was used (Spitler and Bernier, 2016):

$$\overline{\Delta T}(t_n) = \sum_{i=1}^{n} \frac{q_i - q_{i-1}}{2\pi k}\ fls(\alpha, r,\ t_n - t_i, H, D) \qquad (8)$$

where q_i is the linear heat extraction from the borehole during the time step *i*.

The temperature on the borehole wall at time t_n was then calculated as:

$$T_b(t_n) = T_b(t_0) - \overline{\Delta T}(t_n) \qquad (9)$$

where $T_b(t_0)$ is the undisturbed ground temperature.

The heat extraction from the borehole q was considered equal to the heat absorbed by the refrigerant at the evaporator of the HP, output of the HP model. The HP model and heat source model are therefore interconnected, and their solution should be found iteratively. To avoid iterating we assumed T_{sf} as a function of the heat extracted from the borehole during the previous hour $q(t_{n-1})$, rather than the current hour $q(t_n)$, and during the first hour of simulation we calculated T_{sf} as $T_{sf} = T_b - 3$.

The borehole and ground characteristic used for the case study are shown in table 1.

Table 1. Borehole and ground characteristics						
Borehole properties			**Ground properties**			
Length, H [m]	**Buried depth, D [m]**	**Radius, r [cm]**	**Conductivity, k [W/m/K]**	**Density [kg/m^3]**	**Specific heat [J/kg/K]**	**Undisturbed Temperature, $T_b(t_0)$ [°C]**
100	6	0.575	3,1	2300	870	8

2.2 Scenario B: GSHPs in an indefinitely extended neighbourhood

2.2.1 Neighbourhood characteristics

In this scenario, we considered a neighbourhood where all the houses have a GSHP installation identical to the installation considered in Scenario A. The BHEs of the installations are arranged in a square grid, and distant 20 m from the immediately close neighbours, as shown in figure 1. When the operational time considered is 25 years, an indefinitely extended neighbourhood of boreholes having the characteristics as in this study can be approximated to a neighbourhood having a radius of 120 m (figure 2). The approximation holds if the temperatures of all the borehole walls of the BHEs of the infinite neighbourhood are assumed equal to the temperature of the borehole wall of the central BHE of the finite neighbourhood. An explanation for this approximation can be found in Fascì et al. (2019).

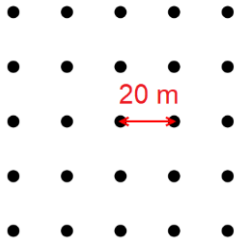


Figure 1: indefinetely extended neighbourhood

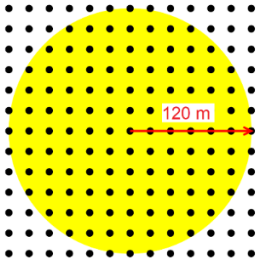


Figure 2: finite neighbourhood approximating the indefinetely extended neighbourhood

2.2.2 Heat source model

Due to the thermal influence between neighbouring boreholes, equation 9 does not hold for Scenario B. It is replaced by equation 10:

$$T_b(t_n) = T_b(t_0) - \overline{\Delta T}(t_n) - \sum_{j=1}^{N\ neighbours} \frac{q_j}{2\pi k} \cdot fls(\alpha, d_j, \widehat{t_n}, H, D) = T_b(t_0) - \overline{\Delta T}(t_n) - \overline{\Delta T}_n(\widehat{t_n}) \quad (10)$$

The term $\overline{\Delta T}_n(\widehat{t_n}) = \sum_{j=1}^{N\ neighbours} \frac{q_j}{2\pi k} \cdot fls(\alpha, d_j, \widehat{t_n}, H, D)$ accounts for the presence of the neighbouring boreholes. $N\ neighbours$ is the number of BHEs surrounding the central BHE, q_j is the average heat extraction from the borehole j during the year, and d_j is the distance between the central borehole and the j[th] borehole. Although the load on each neighbouring borehole varies from hour to hour, this variation is not perceivable after a certain distance, and the temperature change in the underground is approximately the same as if the load were constant and equal to its average value (Fascì at al., 2018). Fascì et al. (2018) have found that beyond 20 m (the minimum distance assumed in this study) the load variation can be considered negligible. Therefore, the term $\overline{\Delta T}_n(\widehat{t_n})$ is calculated assuming constant load. Moreover, the influence of the neighbouring boreholes does not vary significantly between two consecutive years (figure 3), therefore the term $\overline{\Delta T}_n(\widehat{t_n})$ was calculated only once for each year and assumed constant during the wholce year. The time $\widehat{t_n}$at which the term $\overline{\Delta T}_n(\widehat{t_n})$ is calculated was arbitrarily chosen as the first hour of each year.

3. RESULTS AND DISCUSSION

In this section, we show and compare the results obtained simulating Scenario A (Single House) and Scenario B (Neighbourhood).

Since the characteristics of the load are the same in both the scenarios developed, the differences between the performances of the GSHPs of the two scenarios depend only on the differences between the temperatures of the heat sources. These are shown in figures 3 and 4. Figure 3 shows the annual-mean temperature at the borehole wall. Figure 4 shows the hourly temperature of the secondary fluid after circulating in the BHE, for the first and last two years of simulation.

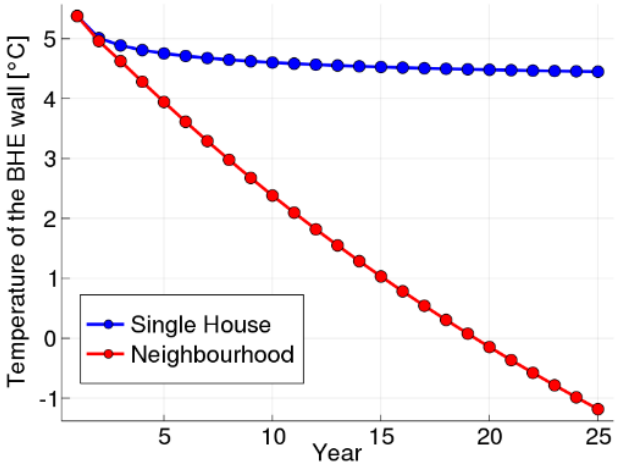


Figure 3: Temperature at the BHE wall

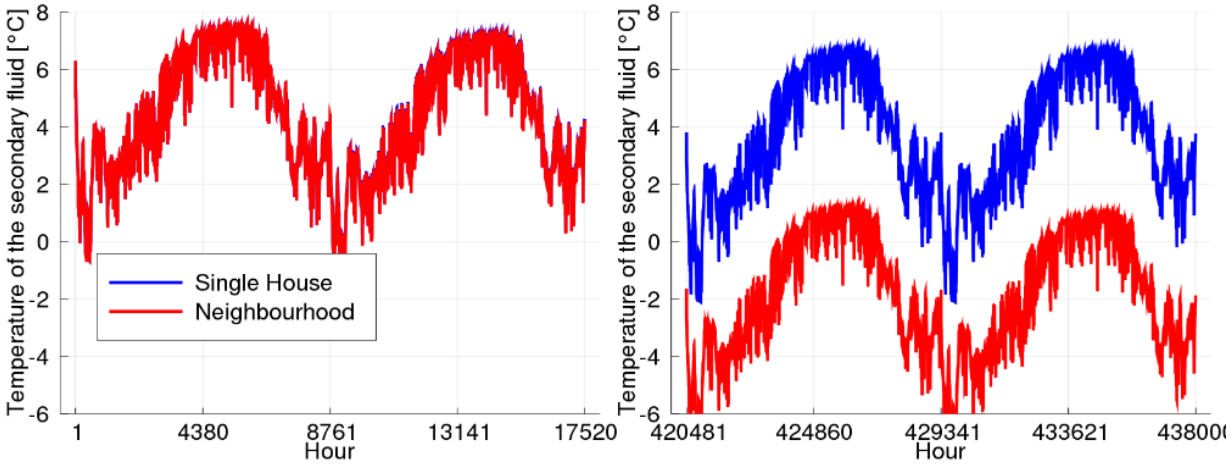


Figure 4: Temperature of the secondary fluid at the outlet of the BHE during the 1st and 2nd years operation (left) and 24th and 25th years of operations (right).

Figure 3 shows that, in Scenario A, the temperature at the borehole wall decreases from an average of 5.4 °C during the first year of operation to 4.5 °C during the 25th year of operation, a decrease of 0.9 K. On the other side, in Scenario B, the temperature at the borehole wall decreases from an average of 5.4 °C during the first year of operation to -1.2 °C during the 25th year of operation, a decrease of 6.6 K. Moreover, in Scenario A the temperature approaches a steady-state condition, however, in Scenario B the temperature does not approach a steady-state condition. This means that if the operation of the GSHP were extended beyond 25 years the working conditions for the GSHP of Scenario A would be steady, while the working conditions for the GSHP of Scenario B would become even worse than the conditions presented in this paper. However, it should be remembered that in this paper we modelled an indefinitely extended neighbourhood; in such a case a steady-state condition would never be reached. However, in reality neighbourhoods have a finite extension, therefore a steady-state condition would be reached. How long it would take to reach the steady-state condition depends on the size of the neighbourhood itself. We also want to underline that in Scenario B the mean temperature at the borehole wall falls below 0 °C after 20 years of operation. Temperatures below 0 °C can lead to freezing of the borehole and damages to the heat exchanger that would comprise the operation of the whole system. The effect of this was not considered in the present study. However, freezing of the ground regularly occurs in Sweden, and it was reported that very few problems are encountered due to this (Ahlström, 2004).

The decrease of the borehole wall temperature shown in figure 3 leads to the decrease of the temperature of the secondary fluid after circulating in the borehole heat exchanger, shown in figure 4. Figure 4 shows that in scenario A, the minimum temperature of the secondary fluid decreases from -0.7 °C during the 1st year to -2.1 °C during the 25th year of operation. In Scenario B, it drops from -0.7 C to -7 °C during the same time span. During the 25th year of operation, on average, the temperature of the secondary fluid in Scenario B is 9 K lower than the in Scenario A.

The decrease of the temperatures of the secondary fluid leads to an increase of the temperature lift of the heat pump and therefore to a decrease of the coefficient of performance (COP) of the system. Figure 5 shows the annual average COP (SCOP) of the GSHPs in Scenario A and Scenario B.

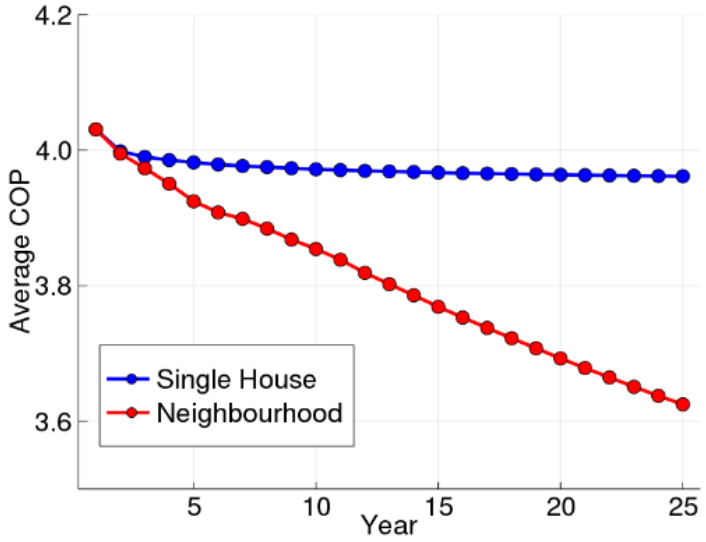


Figure 5: Coefficient of performance (COP) of the heat pump

In Scenario A the SCOP of the HP decreases from 4.03 to 3.96 (1.7%) during the first 25 years of operation and reaches a steady-state condition. During the same time span, in Scenario B, the COP drops from 4.03 to 3.62 (10.2%); moreover, a steady-state condition is not reached.

The decrease of the COP leads to an increase of electricity consumption, both by the compressor of the HP and by the auxiliary heating systems. This is shown in figure 6.

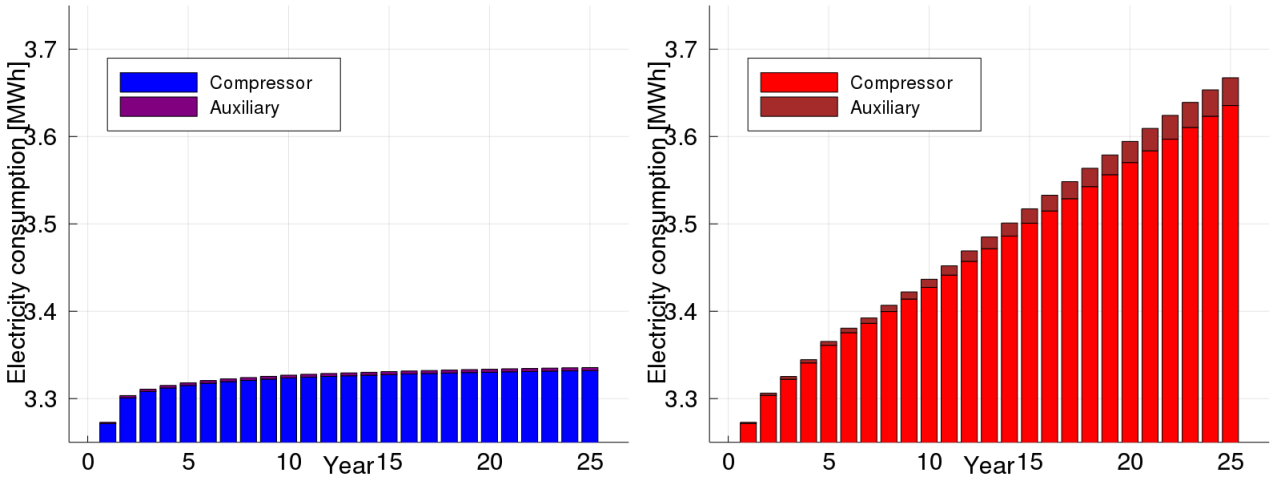


Figure 6: Electricity consumption of the compressor of the HP and auxiliary system for the single house (left) and the house in a densely populated neighbourhood (right)

Figure 6 shows that in Scenario A the annual electricity consumption of the compressor increases from 3.27 MWh to 3.33 MWh (1.8 %) and the electricity consumption of the auxiliary system increases from 1.3 kWh to 3.5 kWh (192 %) during 25 years. In scenario B the electricity consumption of the compressor increases from 3.27 MWh to 3.63 MWh (11 %) and the electricity consumption of the auxiliary system increases from 1.3 kWh to 31.7 kWh (almost 25 times higher). During the 25 years considered, the electricity consumption of the heating system of Scenario B is 3.96 MWh higher than the electricity consumption of the heating system of Scenario A.

Through a rough economic analysis, it may be observed that since the electricity price in Sweden is around 0.2 euro/ kWh (Statista, 2019) the extra consumption of 3.96 MWh corresponds to an extra expense of around 800 euros. Considering that the installation cost of a GSHP in Sweden ranges from 13000-22000 euro and it is supposed to be paid back in 7-8 years (Vattenfall, 2019), the extra expense does not seem to make the investment on a GSHP in Scenario B significantly less advantageous than in Scenario A.

However, from figure 6 we noticed that the auxiliary system has a very low impact on the electricity consumption in both scenarios. In figure 7, we show how often the auxiliary system is used.

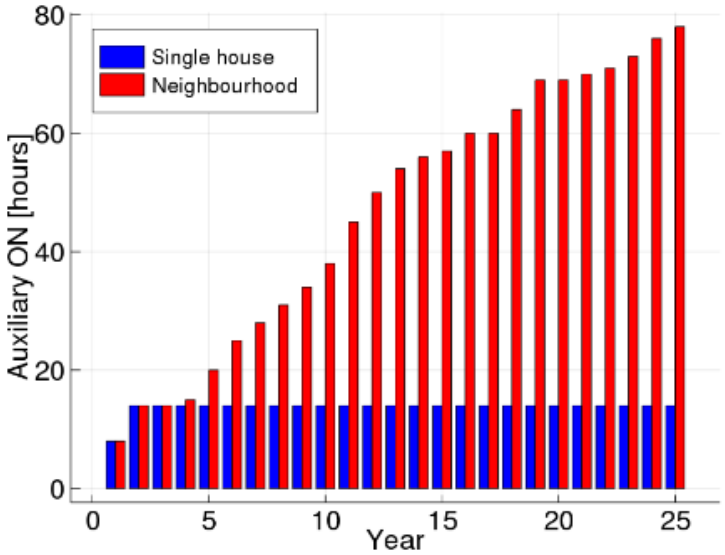


Figure 7: Hours during which the auxiliary heating system is used.

In Scenario A the auxiliary system is used only 8 hours during the 1st year and 14 hours during the 25th year. In Scenario B the auxiliary system is used only 8 hours during the 1st year and 78 hours during the 25th year. In our scenarios, the auxiliary system is used less than in an average Swedish scenario. Indeed, typically GSHPs in Sweden are designed to work under the conditions of Scenario A and to be able to satisfy 80% of the house load under the worst conditions. However, in Scenario A the GSHP was always able to satisfy at least 92% of the load. This means that a smaller HP would be in reality used to satisfy the load we have imposed. Using a smaller HP would lead to a significant increase of the auxiliary system in Scenario B and therefore to an increase of the extra expense of Scenario B compared to Scenario A. The extent of this increase will be study of a further evaluation.

Finally, in figure 8, we show the trend of the heat extracted from the borehole annually.

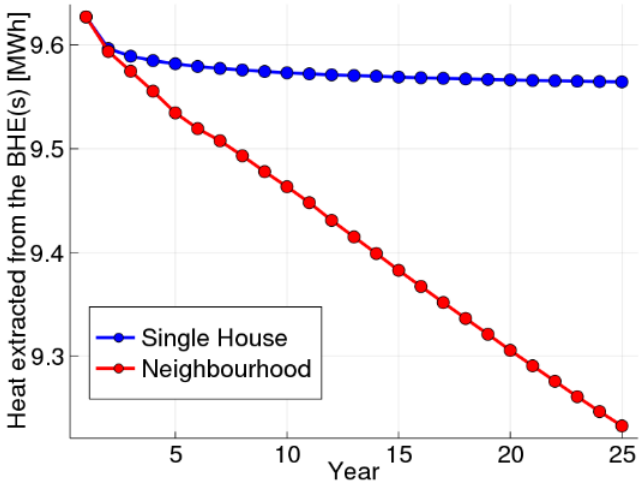


Figure 8: Heat extraction from the borehole heat exchanger(s) (BHE(s))

Figure 8 shows that the heat extraction from the borehole decreases in both scenario; this is due to the reduction of the COP of the systems. In particular, in Scenario A the heat extracted decreases from 9.63 MWh during the first year to 9.56 MWh during the 25th year (0.7 %). In Scenario B the heat extracted decreases from 9.63 MWh during the first year to 9.23 MWh during the 25th year (4.2 %).

Therefore, when the temperature on the borehole wall of a GSHP decreases, the HP lowers the heat extraction and therefore limits the temperature reduction. However, as seen in figure 3 this effect is limited.

4. CONCLUSIONS

In this paper, we have showed a methodology to evaluate the performance of a ground-source heat pump in an area with a high density of similar installations. It should be noticed that the model relies on the assumption of uniform underground properties in a big volume of ground. Therefore, it might be suitable for certain neighbourhoods while unsuitable for others.

We have also applied the methodology to a case study relevant for the Swedish conditions. In our case study, the COP of the system declined of around 10% after 25 years of operation and the electricity consumption increased of around 11%. However, the decrease in performance does not seem to undermine the profitability of the system. Nevertheless, we have noticed that after 20 years of operation the mean-annual underground temperature would drop below 0 °C, this might lead to failures of the system that we have not taken into account; however, considered the past experience failure of the systems due to ground freezing is not likely in Sweden.

In our case study, we have considered installations that start operating simultaneously. The techno-economic analysis of a new installation surrounded by installations that have been operating for several years might lead to completely different results. Finally, the HP we have considered in our case study was slightly oversized for the heating load considered, compared to a usual Swedish installation. A smaller HP would undergo a higher decrease in performance. Therefore, future studies should consider more scenarios to get an exhaustive view on the situation.

Finally, we want to point out that no suitable measures from real installations are available to us to compare the real trend in system performance with the trend forecasted with our model.

ACKNOWLEDGMENTS

This work was supported by the Swedish Energy Agency (Energimyndigheten) under grant number P43647-1.

REFERENCES

Ahlström, A.-K.: Bergvärmeanläggningar där frysning i borrhål orsakar hopklämda kollektorslangar, Master Thesis, Sweden (2004).

Bezanson, J., Edelman, A., Karpinski, S., Shah, VB.: *Julia: A Fresh Approach to Numerical Computing.* SIAM Rev., **59(1),** (2017), 65–98. https://doi.org/10.1137/141000671.

Choi, W., Ooka, R., Nam, Y.: Impact of long-term operation of ground-source heat pump on subsurface thermal state in urban areas. *Sustainable Cities and Society*, **38**, (2018), 429–439. https://doi.org/10.1016/j.scs.2017.12.036

Cimmino, M., and Wetter, M.: Modelling of Heat Pumps with Calibrated Parameters Based on Manufacturer Data, *Proceedings,* The 12th International Modelica Conference, Prague, Czech Republic, May 15-17, (2017), pp. 219–226. https://doi.org/10.3384/ecp17132219

Coronado, M.: Modelling the performance of heat pump systems for single-family houses applications. Not published yet.

Fascì, M. L., Lazzarotto, A., Acuna, J., and Claesson, J.: Thermal influence of neighbouring GSHP installations: relevance of heat load temporal resolution, *Proceedings,* IGSHPA Research Track, Stockholm, Sweden (2018). https://doi.org/10.22488/okstate.18.000019

Fascì, M.L., and Lazzarotto, A.: A novel model for the estimation of thermal influence of neighbouring borehole heat exchangers, *Proceedings,* European Geothermal Congress 2019, The Hague, Netherlands (2019).

Fascì, M. L., Lazzarotto, A., Acuna, J., and Claesson, J.: Analysis of the thermal interference between ground source heat pump systems in dense neighbourhoods. Accepted for publication in *Science and Technology for the Built Environment* in June 2019.

Gehlin, S., and Andersson O.: Geothermal Energy Use, Country Update for Sweden, *Proceedings,* European Geothermal Congress 2016, Strasbourg, France (2016).

Javed, S., Spitler, J.D.: 3 - Calculation of borehole thermal resistance, *Book*, Rees, S.J. (Ed.), Advances in Ground-Source Heat Pump Systems. Woodhead Publishing, (2016), pp. 63–95. https://doi.org/10.1016/B978-0-08-100311-4.00003-0

Jin, H., and Spitler, J.D.: A Parameter Estimation Based Model of Water-To-Water Heat Pumps for use in Energy Calculation Programs. *ASHRAE Transactions*. **108(1)**, (2002), 3-17.

Koohi-Fayegh, S., Rosen, M.A.: An analytical approach to evaluating the effect of thermal interaction of geothermal heat exchangers on ground heat pump efficiency. *Energy Conversion and Management,* **78**, (2014), 184–192. https://doi.org/10.1016/j.enconman.2013.09.064

Miglani, S., Orehounig, K., Carmeliet, J.: A methodology to calculate long-term shallow geothermal energy potential for an urban neighbourhood, *Energy and Buildings*, **159**, (2018), 462-473.

Sanner, B.: 2016.: Shallow geothermal energy–history, development, current status, and future prospects, *Proceedings,* European Geothermal Congress 2016, Strasbourg, France (2016).

Scarpa, M., Emmi, G., and De Carli, M.: Validation of a numerical model aimed at the estimation of performance of vapor compression based heat pumps. *Energy and Buildings*, **47**, (2012), 411-420.

Spitler, J.D. and Bernier, M.: Vertical borehole ground heat exchanger design methods, *Book*, S.J. Rees Advances in Ground-Source Heat Pump Systems. London: Woodhead Publishing, (2016.)

Staffell, I., Brett, D., Brandon, N., & Hawkes, A.: A review of domestic heat pumps. *Energy & Environmental Science*, ***5*(11)**, (2012), 9291-9306.

Statista: Electricity prices for households in Sweden from 2010 to 2018, semi-annually (in euro cents per kilowatt-hour), *Webpage,* https://www.statista.com/statistics/418124/electricity-prices-for-households-in-sweden/, accessed the 24th July 2019.

Vattenfall: Prisexempel för bergvärme, *Webpage, https://www.vattenfall.se/varmepumpar/bergvarme/pris/*, accessed the 24th July 2019.

Witte, H.J.L.: A Novel Tool for Assessing Negative Temperature Interactions between Neighbouring Borehole Heat Exchanger Systems*, Proceedings,* 14th international conference on energy storage, Adana, Turkey (2018).

APPENDIX

Manufacturer data of the HP

Table 2: Performance map of the HP – Heating capacity as a function of the water inlet temperature at the condenser and secondary fluid inlet temperature at the evaporator

		Inlet Temperature at the condenser [°C]				
		30	35	40	45	
Inlet temperature at the evaporator [°C]	5	5.4	5.1	4.9	4.6	Heating Capacity [kW]
	6	5.5	5.3	5.0	4.7	
	7	5.7	5.5	5.2	4.9	
	8	5.9	5.6	5.3	5.0	
	9	6.1	5.8	5.5	5.2	
	10	6.3	6.0	5.7	5.3	

Table 3: Performance map of the HP – Compressor power as a function of the water inlet temperature at the condenser and secondary fluid inlet temperature at the evaporator

		Inlet Temperature at the condenser [°C]				
		30	35	40	45	
Inlet temperature at the evaporator [°C]	5	1.4	1.6	1.8	2.0	Compressor Power [kW]
	6	1.4	1.6	1.8	2.0	
	7	1.4	1.6	1.8	2.0	
	8	1.4	1.6	1.8	2.0	
	9	1.4	1.6	1.8	2.0	
	10	1.4	1.6	1.8	2.1	

- Water flow rate in the condenser: 1451 kg h^{-1}
- Secondary fluid flow rate at the evaporator: 563 kg h^{-1}

Optimized Parameters of the HP:

- **Volume ratio: Vr** = 2.52 [-]
- **Nominal refrigerant volume flow rate: V** = 0.00123 [m^3/s]
- **Leakage coefficient: C** = 0.00026 [kg/s]
- **Degree of superheating: ΔT_{sup}** = 5.7 [K]
- **Compressor efficiency: η** = 0.94 [-]
- **Compressor constant losses: W_{loss} =** 130 [W]
- **Heat transfer coefficient of the evaporator: UA_{eva}** = 2881 [W/K]
- **Heat transfer coefficient of the condenser: UA_{cond}** = 3286 [W/K]